

Big bang nucleosynthesis and early dark energy in light of the EMPRESS Y_p results and the H_0 tension

Tomo Takahashi¹ and Sora Yamashita²

¹*Department of Physics, Saga University, Saga 840-8502, Japan*

²*Graduate School of Science and Engineering, Saga University, Saga 840-8502, Japan*

Abstract

Recent measurement of the primordial ${}^4\text{He}$ abundance Y_p from EMPRESS suggests a cosmological scenario with the effective number of neutrino species deviated from the standard value and non-zero lepton asymmetry. We argue that the extension of the standard cosmological model would be more demanded when the Hubble tension is taken into account, in which derived baryon density could be somewhat higher than the standard ΛCDM framework. We also discuss the issue by assuming early dark energy whose energy density can have a sizable fraction at the epoch of big bang nucleosynthesis. We show that the existence of early dark energy can reduce some tension implied by the EMPRESS Y_p results.

1 Introduction

The concordance model of cosmology has now been established, which can successfully explain various cosmological observations almost consistently, which is the so-called Λ CDM model. However, in recent years, several tensions in the framework of Λ CDM have been under debate, which may suggest a modification/extension of the concordance Λ CDM model. One of them is the Hubble tension (the H_0 tension) where there is a discrepancy in the values of the Hubble constant H_0 measured directly in the local Universe and indirectly from such as cosmic microwave background (CMB) in the framework of Λ CDM. More specifically, the Cepheid calibrated supernova distance ladder measurement gives $H_0 = 73.04 \pm 1.04$ km/s/Mpc [1], on the other hand, CMB data from Planck in combination with baryon acoustic oscillation (BAO) measurements infers $H_0 = 67.66 \pm 0.42$ km/s/Mpc [2], which are discrepant at 4.8σ level. Even without CMB data, the tension between direct and indirect measurements still persists [3–5] and indeed other direct and indirect measurements also show a similar tendency for each category (see, e.g., [6, 7] for a review), which motivates many works to resolve the tension and pursue models beyond the standard Λ CDM (see, e.g., [6, 8] for a review).

Another issue has appeared recently from the measurement of the primordial ${}^4\text{He}$ abundance Y_p by Extremely Metal-Poor Representatives Explored by the Subaru Survey (EM-PRESS) which obtained $Y_p = 0.2379^{+0.0031}_{-0.0030}$ [9]. This value is somewhat smaller than the previously obtained ones such as Aver et al., $Y_p = 0.2449 \pm 0.0040$ [10], Hsyu et al., $Y_p = 0.2436^{+0.0039}_{-0.0040}$ [11], and Kurichin et al., $Y_p = 0.2462 \pm 0.0022$ [12]. Actually, by combining the measurement of the deuterium abundance D_p from Cooke et al. [13], $D_p = (2.527 \pm 0.030) \times 10^{-5}$, the EMPRESS results give constraints on the effective number of neutrino species $N_{\text{eff}} = 2.41^{+0.19}_{-0.21}$ and the baryon-to-photon ratio $\eta \times 10^{10} = 5.80^{+0.15}_{-0.13}$ [9] in the framework of Λ CDM+ N_{eff} model. The value of N_{eff} deviates from the standard one^{#1} and the baryon-to-photon ratio is slightly smaller than that obtained from Planck in the framework of the Λ CDM model. This may raise another tension in the standard cosmological model, which is referred to as the “Helium anomaly” in some literature.

Actually when one introduces a non-zero chemical potential for electron neutrino μ_{ν_e} which is commonly characterized by the degeneracy parameter $\xi_e = \mu_{\nu_e}/T$ with T being the neutrino temperature, one obtains $\xi_e = 0.05^{+0.03}_{-0.03}$ and $N_{\text{eff}} = 3.22^{+0.33}_{-0.32}$ [9] with a Gaussian prior for the baryon-to-photon ratio $\eta \times 10^{10} = 6.132 \pm 0.038$ motivated by the Planck result in the Λ CDM framework [2]^{#2}. This suggests a non-zero lepton asymmetry, and its implications have been discussed in [21–24]. Instead of invoking a non-zero lepton asymmetry, one can also envisage a model with modified gravity [25] to resolve the helium anomaly. In any case, the EMPRESS result may indicate that we need a model beyond the standard paradigm and pose yet another tension in cosmology.

Actually, as we will argue in this paper when the Hubble tension is taken into account,

^{#1}Although we use $N_{\text{eff}} = 3.046$ [14] as a reference value for the standard case, recent precise calculations give $N_{\text{eff}} = 3.044 - 3.045$ [15–19].

^{#2}See [20] for the implication of non-zero lepton asymmetry and extra radiation for the H_0 tension.

the above EMPRESS result would imply a non-standard scenario even more. In many attempts to explain the H_0 tension, it can be resolved in such a way that the value of H_0 derived indirectly from the data of CMB, BAO and so on gets higher and becomes close to the one from the direct measurements. Indeed the baryon density obtained in such model frameworks tends to be affected and becomes higher than the value in the Λ CDM case, which makes the above-mentioned discrepancy more severe. We discuss this issue quantitatively by investigating the fit to the EMPRESS Y_p result in combination with deuterium abundance from [13] with the prior for baryon density suggested by the H_0 tension.

Moreover, we also argue that one can reduce the degree of the helium anomaly by extending the standard model by introducing early dark energy (EDE) model [26] which has been extensively discussed in the context of the H_0 tension (for various works of EDE, see, e.g., [6]). Although the EDE model we consider in this paper has an energy scale different from the one introduced to resolve the H_0 tension, the behavior is quite the same in the sense that the energy density of EDE gives a sizable contribution to the total one during the epoch of BBN. Indeed, as we discuss in this paper, we do not need to assume non-zero lepton asymmetry and/or non-standard value of N_{eff} by assuming the existence of EDE in some cases to relax the helium anomaly.

The structure of this paper is as follows. In the next section, we discuss the implications of the Hubble tension to BBN, particularly focusing on its consequences on the EMPRESS Y_p results through the value of baryon density suggested by models which may resolve the H_0 tension. Then in Section 3, we argue that, by introducing EDE whose energy fraction becomes relatively large during the BBN era, the anomaly implied by the EMPRESS results can be alleviated. In the final section, we conclude our paper.

2 Implications of the Hubble tension to BBN

In this section, we discuss the implication of the H_0 tension to BBN, especially focusing on the effect of the prior on baryon density suggested by the tension. In Table 1, we list the constraints on the baryon density $\Omega_b h^2$ in the Λ CDM and example models proposed to resolve the H_0 tension. As such example models, most of them are taken from among those referred as “successful” models as a possible solution to the H_0 tension in [8] based on the criteria of the Gaussian tension, the difference of the maximum a posteriori and the Akaike information criterium (see Table 1 in [8]). We have taken the constraints on $\Omega_b h^2$ from the references cited in the last column of Table 1. We should note that the dataset used in the analysis of those references differs, and currently, there is no consensus on which model is more plausible, and hence the values quoted in the table can be regarded as just a reference. Nevertheless, we can clearly see that, in models proposed as a solution to the H_0 tension, the value of $\Omega_b h^2$ tends to be higher than the one in the Λ CDM model, which shows that the H_0 tension would have yet another impact on cosmology^{#3}.

^{#3}Other implications of the H_0 tension to other aspects of cosmology have been discussed such as cosmological bounds on neutrino masses [27] and the scale dependence of primordial power spectrum [28–31].

| Model | $100\Omega_b h^2$ | η_{10} | H_0 | Dataset | Ref. |
|---|---------------------------|--------------------------|-------------------------|---------|------|
| Λ CDM | 2.242 ± 0.014 | 6.14 ± 0.038 | 67.66 ± 0.42 | (a) | [2] |
| Varying $m_e + \Omega_k$ | $2.365^{+0.033}_{-0.037}$ | $6.48^{+0.090}_{-0.101}$ | $72.84^{+1.0}_{-1.0}$ | (b) | [34] |
| Early dark energy ($\phi^4 + \text{AdS}$) | $2.346^{+0.017}_{-0.016}$ | $6.42^{+0.047}_{-0.044}$ | $72.64^{+0.57}_{-0.64}$ | (b) | [35] |
| Early dark energy (axion type) | 2.285 ± 0.021 | 6.26 ± 0.057 | $70.75^{+1.05}_{-1.09}$ | (c) | [36] |
| New early dark energy | $2.292^{+0.022}_{-0.024}$ | $6.27^{+0.060}_{-0.066}$ | $71.4^{+1.0}_{-1.0}$ | (d) | [37] |
| Early modified gravity | 2.275 ± 0.018 | 6.23 ± 0.049 | 71.21 ± 0.93 | (e) | [38] |
| Primordial magnetic field | 2.266 ± 0.014 | 6.20 ± 0.038 | 70.57 ± 0.61 | (f) | [39] |
| Majoron | 2.267 ± 0.017 | 6.21 ± 0.047 | 70.18 ± 0.61 | (a) | [40] |

Table 1: Constraints on the baryon density $\Omega_b h^2$ and its corresponding baryon-to-photon ratio η_{10} in models proposed to resolve the H_0 tension. For the dataset shown in the 5th column (a)–(f) denotes: (a) Planck 2018 + BAO, (b) Planck 2018 + BAO + SN + H_0 , (c) Planck 2018 + BAO + SN + H_0 + RSD + DES, (d) Planck 2018 + BAO + SN + BBN + H_0 , (e) Planck 2018 + SN + H_0 and (f) Planck 2018 + BAO + SN + DES + H_0 . Here “Planck 2018” refers to Planck 2018 TT, TE, EE + lensing, and “ H_0 ” indicates that the analysis adopts the H_0 prior with the value motivated by a direct local measurement such as the one from distance ladder observations. For details of the analysis, see the references shown in the last column. We should note that most analyses quoted in the table include the H_0 prior, and hence some caution should be taken when interpreting the value of H_0 obtained in the analyses.

Actually, this is somewhat expected since the correlation between $\Omega_b h^2$ and H_0 in the position and height of acoustic oscillations in CMB angular power spectrum has already been known (see, e.g., [32, 33]) although it becomes somewhat involved in models where the H_0 tension can be solved. To resolve the tension, one needs to reduce the sound horizon at recombination r_s , but also has to keep CMB angular power spectra almost intact to obtain a good fit to CMB data (and also to BAO). For example, in time-varying electron mass model [34], one can reduce r_s by slightly raising the electron mass m_e at recombination epoch, however, to keep a good fit to CMB, the baryon density $\Omega_b h^2$ should also be increased in accordance with the change of m_e as $\delta m_e / m_e = \delta(\Omega_b h^2) / \Omega_b h^2$ (see Ref. [34] for detailed discussion). Also in the early dark energy model, in order to increase the value of H_0 , one needs to shift $\Omega_b h^2$ to a higher value to have the CMB angular power spectrum almost the same, which can be realized by keeping the acoustic scale and angular damping scale almost unchanged (for details, see, e.g., [28]).

When one discusses BBN, the baryon density is usually quoted by the baryon-to-photon ratio $\eta = n_b / n_\gamma$ with n_b and n_γ being the number densities of baryon and photon. The conversion factor from the baryon density $\Omega_b h^2$ to the baryon-to-photon ratio $\eta_{10} = 10^{10} \eta$ is given by [41] (see also, e.g., [42, 43])

$$\eta_{10} = \frac{273.279}{1 - 0.007125 Y_p} \left(\frac{2.7255 \text{ K}}{T_{\gamma 0}} \right)^3 \Omega_b h^2, \quad (2.1)$$

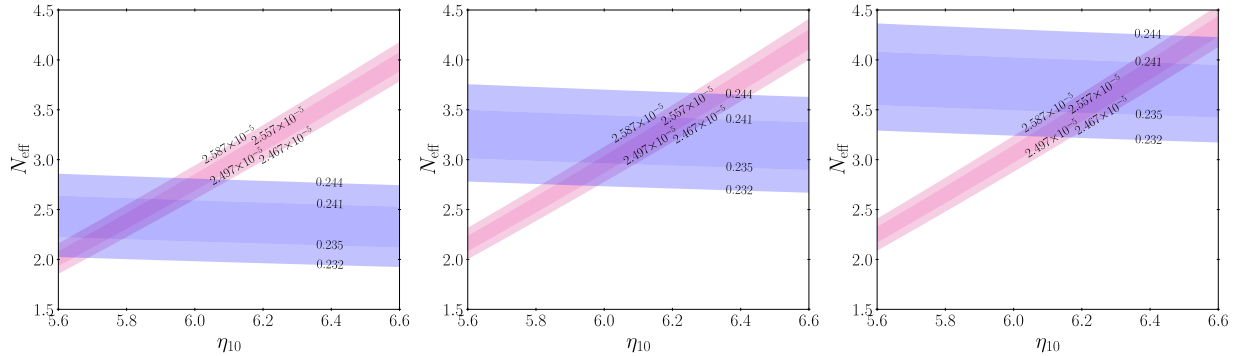


Figure 1: 1σ and 2σ allowed regions for Y_p [9] (light and dark blue regions for 1σ and 2σ) and D_p [13] (light and dark magenta regions for 1σ and 2σ) in the η_{10} - N_{eff} plane. We take the neutrino degeneracy parameter as $\xi_e = 0$ (left), 0.05 (middle) and 0.08 (right).

where $T_{\gamma 0}$ is the present photon temperature. Precisely speaking, the conversion factor depends on the primordial helium abundance. Although we have adopted the EMPRESS mean value of $Y_p = 0.2379$ to obtain η_{10} , the dependence on Y_p is very weak so that its uncertainty can be neglected compared to the error in $\Omega_b h^2$ obtained from CMB, and hence the actual value of Y_p in Eq. (2.1) scarcely affects the following argument. We also list the value of η_{10} derived by using Eq. (2.1) for each model in Table 1. As seen from the table, models proposed to resolve the H_0 tension tend to suggest a higher value of η_{10} compared to the one in Λ CDM. In some cases, the mean value of η_{10} can be high as $\eta_{10} \sim 6.48$ although, in general, the error is also somewhat larger than that for the Λ CDM case.

Indeed as already argued in [9], the value of Y_p obtained by EMPRESS would imply non-zero lepton asymmetry, which is characterized by non-zero electron neutrino degeneracy parameter ξ_e , and the value of N_{eff} larger than the standard one. This tendency would become more prominent when the baryon density is high, which can be understood from Fig. 1 where 1σ and 2σ allowed region from the measurements of Y_p [9] and D_p [13] are shown in the η_{10} - N_{eff} plane for several values of ξ_e . We use a public code `PARthENoPE` [41, 44, 45] to calculate the helium and deuterium abundances. As seen from the figure, as ξ_e takes more positive values, Y_p decreases [46], which makes higher η_{10} more preferred from the combination of the EMPRESS Y_p results [9] and D_p from [13]. This indicates that when a higher value of baryon density is favored from CMB, which can be taken into account in the analysis as a prior for η_{10} as will be done in the following, a more (positively) non-zero value of ξ_e and N_{eff} higher than the standard value are more preferred.

To discuss the implication of a high value of η_{10} suggested by the H_0 tension in a more quantitative manner, we investigate a constraint in the N_{eff} - ξ_e plane from the helium abundance Y_p of EMPRESS [9] and deuterium D_p [13] with the prior for baryon-to-photon ra-

tio η_{10} . To obtain the constraint, we calculate χ^2 as

$$\chi^2 = \frac{(Y_p^{\text{obs}} - Y_p^{\text{th}})^2}{\sigma_{Y_p, \text{obs}}^2 + \sigma_{Y_p, \text{sys}}^2} + \frac{(D_p^{\text{obs}} - D_p^{\text{th}})^2}{\sigma_{D_p, \text{obs}}^2 + \sigma_{D_p, \text{sys}}^2} + \frac{(\eta_{10}^{\text{ref}} - \eta_{10})^2}{\sigma_{\eta_{10}}^2}, \quad (2.2)$$

where we adopt $Y_p^{\text{obs}} = 0.2379$, $\sigma_{Y_p, \text{obs}} = 0.0031$ [9] and $D_p^{\text{obs}} = 2.527 \times 10^{-5}$, $\sigma_{D_p}^{\text{obs}} = 0.030 \times 10^{-5}$ [13] for helium and deuterium abundances, respectively. We also include the errors in the theoretical calculation for helium as $\sigma_{Y_p, \text{sys}}^2 = (0.0003)^2 + (0.00012)^2$ where the first and second errors come from the uncertainties on nuclear rate and neutron decay rate with $\tau_n = 879.4 \pm 0.6$ sec [47], respectively [45]. For deuterium, we adopt $\sigma_{D_p, \text{sys}}^2 = (0.05 \times 10^{-5})^2$ coming from nuclear rate uncertainties [45]. Y_p^{th} and D_p^{th} are theoretically predicted values for given model parameters such as η_{10} , N_{eff} and ξ_e . When we vary the baryon density η_{10} in the analysis, we add the third term to evaluate the value of χ^2 .

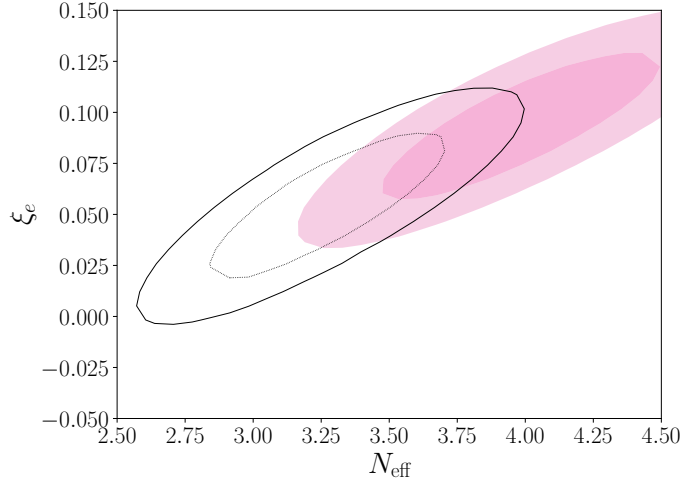


Figure 2: 1σ and 2σ allowed region in the $N_{\text{eff}}-\xi_e$ plane from measurements of Y_p and D_p with η_{10} prior. For the η_{10} prior, we take $\eta_{10} = \eta_{10}^{\text{ref},1} \pm \sigma_{\eta_{10},1} = 6.14 \pm 0.038$ (black dotted and solid lines for 1σ and 2σ) obtained from CMB+BAO [2] in the Λ CDM framework and $\eta_{10} = \eta_{10}^{\text{ref},2} \pm \sigma_{\eta_{10},2} = 6.4 \pm 0.060$ which is suggested by the H_0 tension (light and dark magenta regions for 1σ and 2σ).

For the baryon density, we consider two priors motivated by the constraints from CMB analysis in the standard Λ CDM and models proposed to solve the H_0 tension and take the following reference values for η_{10}^{ref} and $\sigma_{\eta_{10}}$:

$$\eta_{10}^{\text{ref},1} = 6.14, \quad \sigma_{\eta_{10},1} = 0.038, \quad (2.3)$$

$$\eta_{10}^{\text{ref},2} = 6.40, \quad \sigma_{\eta_{10},2} = 0.060. \quad (2.4)$$

For the case 1, which is motivated by the analysis in the standard Λ CDM framework, we take $\eta_{10}^{\text{ref},1}$ and $\sigma_{\eta_{10},1}$ as the same as the Λ CDM in Table 1. For the case 2, we take the

values motivated from the analysis in models which can resolve the H_0 tension. As seen from Table 1, the mean value of η_{10} varies from model to model, however one can see the tendency that a higher η_{10} is preferred when a model allows a higher value of H_0 . In order that the value of H_0 from indirect measurement such as CMB would be consistent with that obtained from direct measurements, it should be high enough to be close to $H_0 = 73.04 \pm 1.04$ km/s/Mpc [1]. Among the values for H_0 listed in Table 1, the ones in varying $m_e + \Omega_k$ and early dark energy (ϕ^4 +AdS) models are close to it, in which the mean value of the baryon density is $\eta_{10} = 6.48$ and 6.42 , respectively. Motivated by these values, but here we conservatively take $\eta_{10} = 6.40$ for the reference value of the case 2. The uncertainty of η_{10} in those models is somewhat larger than that in the Λ CDM case. We take $\sigma_{\eta_{10,2}} = 0.060$ as the reference value, which corresponds to the average value for the uncertainty of η_{10} listed in Table 1 excluding Λ CDM (rounded up to the second decimal place).

In Fig. 2, we show 1σ and 2σ allowed regions in the $N_{\text{eff}}-\xi_e$ plane obtained by evaluating χ^2 given in Eq. (2.2). From the figure, one can see that when a higher value of η_{10} is assumed for the prior, more positively non-zero lepton asymmetry (non-zero degeneracy parameter for the electron neutrino ξ_e) and larger value of N_{eff} are preferred, which indicates that, in the light of the H_0 , the EMPRESS result on Y_p gives a more pronounced consequence for N_{eff} and the lepton asymmetry (when the previous measurement of Y_p such as from [10–12] is adopted, the allowed ranges for N_{eff} and ξ_e are closer to the standard ones compared to the case using the EMPRESS Y_p).

Here we discussed the implications of a high baryon density, which may be suggested by the H_0 tension, for the EMPRESS Y_p results in the framework where a non-zero lepton asymmetry characterized by ξ_e and a non-standard value of N_{eff} are allowed. Then we showed that a positively large non-zero ξ_e and a larger N_{eff} than the standard case are more preferred. However, we can also consider another framework to discuss the implications of the EMPRESS Y_p results in the light of the H_0 tension. As such an example, we will consider early dark energy model in the next section.

3 Big bang nucleosynthesis with early dark energy

Now in this section, we discuss the impact of early dark energy (EDE), which has been intensively studied in the context of the H_0 tension, on BBN in the light of the EMPRESS result on Y_p . First we present the EDE model considered in this paper, then we investigate constraints on η_{10} , N_{eff} and ξ_e from the EMPRESS Y_p in combination with the measurement of D_p in the existence of EDE.

3.1 Early dark energy

EDE models have been extensively investigated in the context of the H_0 tension, whose typical realization is given by a scalar field ϕ with a potential, for example, such as $V(\phi) =$

$V_0 [1 - \cos(\phi/f)]^n$, with V_0 representing the energy scale, f being a parameter in the model and n controlling the scaling of its energy density after ϕ starts to oscillate. A general behavior of the energy density of EDE ρ_{EDE} is that, when ϕ slowly rolls on the potential in the early times, ρ_{EDE} is almost constant and acts like a cosmological constant, and then, when the effective mass of ϕ becomes the same as the Hubble rate, it starts to oscillate around the minimum of its potential. Around the minimum, the potential can be approximated as $V \propto \phi^{2\alpha}$ and hence, its energy density scales as $\rho_{\text{EDE}} \propto a^{-4}$ for $\alpha = 2$, $\rho_{\text{EDE}} \propto a^{-9/2}$ for $\alpha = 3$, and so on. If EDE starts to oscillate around the epoch of recombination and has some energy fraction at the beginning of its oscillation, EDE affects the evolution of perturbations around recombination, and then soon becomes irrelevant to the evolution of the Universe since ρ_{EDE} dilutes away faster than matter, which is a scenario considered in the context of the H_0 tension. However, here we discuss a case where EDE can have a sizable energy density fraction at some time during BBN.

In the following, we consider two types of EDE: The first one is essentially the same as that adopted to resolve the H_0 tension [26], in which an EDE component behaves like a cosmological constant at early times, and then its energy density quickly dilutes away at some epoch during BBN. As mentioned above, the energy scale of EDE considered here is different from that motivated by the H_0 tension, such an EDE can be realized by assuming appropriate model parameters even for the same potential as the one adopted to resolve the H_0 tension. One could also think of a scenario where two (or more) EDEs are embedded in one framework like in chain early dark energy model [48] in which the Universe experiences multiple first-order phase transitions and some of them act as EDE at BBN and recombination epochs. Another such an example is cascading dark energy [49] where multiple scalar fields can act as dark energy at different eras, which can also accommodate a scenario that EDEs affect the epochs of recombination and BBN such that they relax both the H_0 tension and the helium anomaly.

Here we just assume an EDE which can have a sizable energy fraction at BBN epoch, and then its energy density dilutes quickly, which we describe its evolution of energy density by adopting the following phenomenological model for simplicity and generality such that the description can capture an essential behavior of the model. We model the evolution of the energy density of the first type of EDE, which we refer to as ‘‘EDE1’’ in the following, as

$$\rho_{\text{EDE},1} = \begin{cases} \rho_0 & (T \geq T_t), \\ \rho_0 \left(\frac{T}{T_t}\right)^n & (T < T_t), \end{cases} \quad (3.1)$$

where T is the cosmic temperature and T_t is the transition temperature at which the energy density changes its behavior. n is a parameter which describes the scaling of its energy density. Since the Universe is radiation-dominated during BBN, the temperature essentially scales as $T \propto 1+z \propto 1/a$. ρ_0 is assumed to be constant, and hence it represents the vacuum energy before EDE starts to dilute away. We have modified `PARthENoPE` code [41, 44, 45] to

include the EDE. In the calculation, we actually use the energy fraction of EDE at the time of transition, denoted as f_{EDE} , to control the transition time instead of directly using T_t , which is defined by

$$f_{\text{EDE}} \equiv \frac{\rho_{\text{EDE}}(T_t)}{\rho_{\text{tot}}(T_t)} = \frac{\rho_{\text{EDE}}(T_t)}{\rho_{\text{EDE}}(T_t) + \rho_{rB}(T_t)}, \quad (3.2)$$

where ρ_{tot} is the total energy density including the EDE component and $\rho_{rB}(T)$ is the sum of energy densities of photon, neutrino, electron and baryon. In our calculation, we take account of the time variation of ρ_{rB} properly and set T_t for a given f_{EDE} . One can approximately evaluate T_t for a given f_{EDE} as $T_t \sim 1 \text{ MeV} ((\rho_0/1 \text{ MeV}^4)(1 - f_{\text{EDE}}))^{1/4}$. Since ρ_{rB} monotonically decreases, but ρ_{EDE} is constant when $T > T_t$, the impact of EDE is the largest at around $T = T_t$.

The second type of EDE we consider is the one which behaves as a negative cosmological constant until some time during BBN and it quickly settles down to the observed cosmological constant today. Although EDE having a negative energy density seems somewhat contrived or exotic, such a negative cosmological constant has been investigated in the context of the H_0 tension [35, 50, 51], and the tension in BAO observations at $z \simeq 2.4$ between the ones observed from Lyman α forest and the predicted values in Λ CDM model^{#4} [56, 57]. Furthermore, some theoretical frameworks motivate a negative dark energy such as bimetric gravity [58–60], graduated dark energy [61–63], everpresent Λ [64, 65] and so on. In particular, in the everpresent Λ model, the energy fraction of negative dark energy can have a sizable contribution to the total one at some time due to its stochastic nature [64, 65]. Although one could predict the evolution of such dark energy for a given model, here we assume that the EDE energy density changes from a negative constant to almost zero (actually to a very small value which can explain the present-day dark energy) at some time during BBN. Since a tiny cosmological constant should be negligible compared to other energy components during BBN epoch, to study the effect of this second type of EDE, which we refer to as “EDE2” in the following, we model the energy density of EDE2 simply as

$$\rho_{\text{EDE},2} = \begin{cases} -\rho_0 & (T \geq T_t), \\ 0 & (T < T_t), \end{cases} \quad (3.3)$$

where ρ_0 is a constant, whose value represents the energy density of EDE2 at early time. As in the case of EDE 1, instead of using T_t , we in practice use the energy density fraction of EDE f_{EDE} to specify the time when the transition from $\rho_{\text{EDE},2} = -\rho_0$ to $\rho_{\text{EDE},2} = 0$ occurs in our analysis. Since this kind of EDE can reduce the expansion rate of the Universe at some certain period during BBN, the study of this type of EDE also gives a general insight into models where the expansion rate diminishes at some particular epoch during BBN.

By assuming two types of EDE described above, we discuss the impact of EDE on the abundance of light elements and its implications for the helium anomaly. In particular, we

^{#4}Although the tension has been suggested as $\sim 2\sigma - 2.5\sigma$ [52–54], it is reduced to 1.5σ in a recent measurement [55].

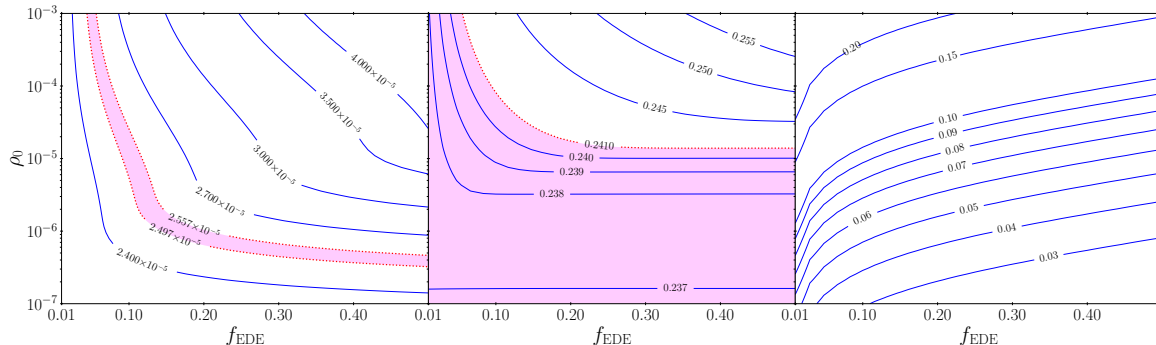


Figure 3: Contours of D_p (left), Y_p (middle) and T_t [MeV] (right) in the $f_{\text{EDE}}-\rho_0$ plane for EDE1 with $n = 4$. 1σ allowed region for Y_p and D_p is shaded with light magenta. The value of ρ_0 is shown in MeV^4 unit. In this figure, we take $\eta_{10} = 6.14$, $N_{\text{eff}} = 2.3$ and $\xi_e = 0$.

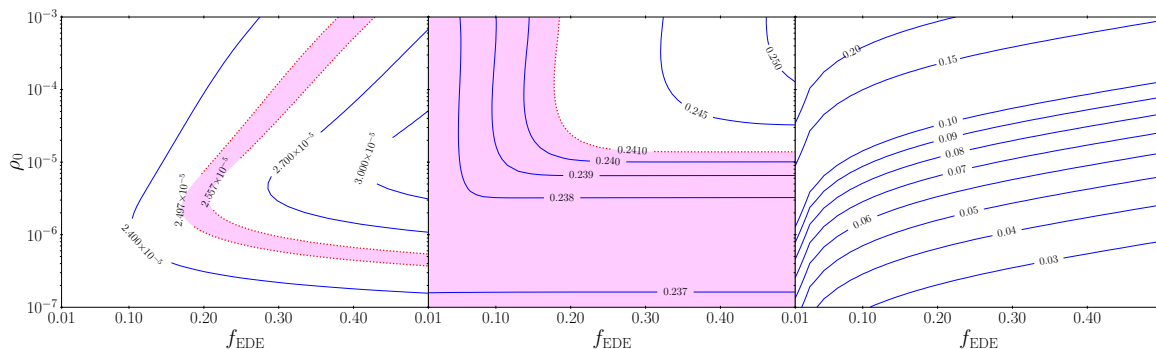


Figure 4: The same as Fig. 3 except that $n = 6$ is assumed in this figure.

investigate constraints on the parameters such as η_{10} , N_{eff} and ξ_e in the presence of EDE to discuss its impact on BBN, which will be presented in the next section.

3.2 Impact of EDE to BBN

Here we discuss how the existence of EDE affects constraints on η_{10} , N_{eff} and ξ_e from the abundances of helium and deuterium, especially in the light of the result from EMPRESS on Y_p and the H_0 tension.

First we show contours of D_p , Y_p and T_t in the $f_{\text{EDE}}-\rho_0$ plane for the EDE1 with $n = 4$ and $n = 6$ cases in Figs. 3 and 4, respectively. Other parameters are taken as $\eta_{10} = 6.14$, $N_{\text{eff}} = 2.3$ and $\xi_e = 0$. The reason why we take $N_{\text{eff}} = 2.3$, which is smaller than the standard value, is that when $N_{\text{eff}} = 3.046$ and $\xi_e = 0$ are assumed, the value of Y_p always larger than the 1σ upper limit obtained by EMPRESS in the ranges of f_{EDE} and ρ_0 shown in the

figure, but by lowering the value of N_{eff} , Y_p gets smaller so that the 1σ allowed range for Y_p becomes visible. Since the existence of EDE affects the abundance of light elements through the change of the expansion rate of the Universe, in which the freeze-out time of nuclear reactions gets modified, the abundances of helium and deuterium change depending on f_{EDE} and ρ_0 . As f_{EDE} or ρ_0 increases (i.e., the effects of EDE becomes larger), the expansion rate gets bigger particularly around $T = T_t$, which makes the neutron freeze-out earlier and hence the value of Y_p increases. The same tendency also holds true for deuterium, which can be seen from the left panel of the figure. It should also be noticed that, in the bottom half region in the middle panel, Y_p scarcely changes even when f_{EDE} is increased. Indeed this region corresponds to the one where the transition temperature is lower than 0.07 MeV as seen from the right panel of the figure. At around this temperature, the helium abundance almost freezes out, below which the value of Y_p would not be affected even if the expansion rate is changed, i.e., the amount of EDE is irrelevant below $T_t \sim 0.07$ MeV. This is the reason why Y_p almost stays constant regardless of the change of f_{EDE} . Compared to Y_p , since the deuterium abundance evolves gradually and does not reach a constant value until late time, D_p decreases continuously against the changes of f_{EDE} and ρ_0 although the response becomes insensitive in the bottom region as in the case of Y_p .

Indeed the cases of $n = 4$ and 6 show almost the same tendencies for both D_p and Y_p (contours for T_t are the same for $n = 4$ and 6 since T_t is the temperature when the energy density of EDE1 changes its behavior which is irrelevant to the scaling of ρ_{EDE1} below $T = T_t$). However, some differences, particularly in D_p , appear in the region above $\rho_0 \gtrsim \mathcal{O}(10^{-6})$ MeV⁴. Since the scaling of the energy density of EDE1 in the $n = 4$ case is the same as that of radiation, it mimics the effects of N_{eff} below $T = T_t$, on the other hand, when $n = 6$, ρ_{EDE} quickly dilutes away and EDE scarcely affect the expansion rate any more. Therefore the difference between the cases with $n = 4$ and 6 only appears when the EDE1 makes a contribution sufficient enough to affect the Hubble expansion rate even for $T < T_t$. However, allowed overlapping regions between Y_p and D_p are almost the same for the $n = 4$ and 6 cases, and the final constraint also becomes almost similar. Therefore we only consider the case of $n = 6$ for EDE1 in the following argument. It should be noted that the energy density of EDE1 with $n = 6$ dilutes faster than radiation and becomes negligible soon below $T = T_t$. Therefore it does not affect the later evolution of the Universe, and such an EDE would only affect the BBN epoch.

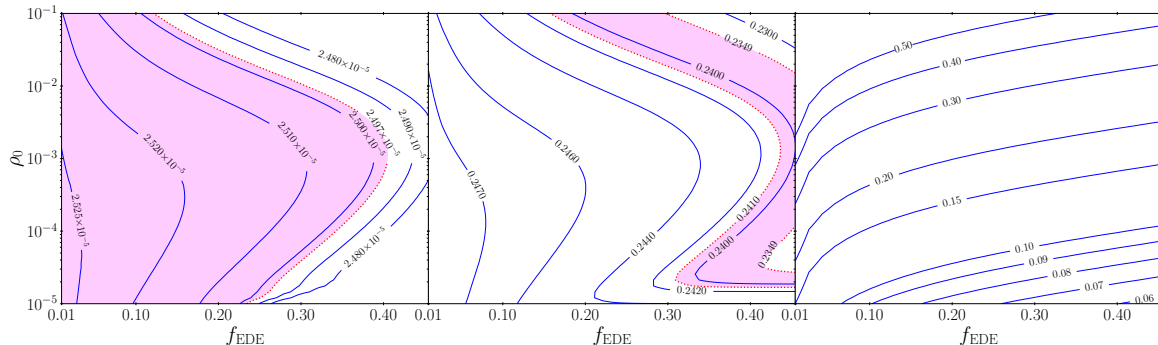


Figure 5: Contours of D_p (left), Y_p (middle) and T_t [MeV] (right) in the $f_{\text{EDE}}-\rho_0$ plane for EDE2. 1σ allowed region for Y_p and D_p is shown with light magenta. The value of ρ_0 is shown in MeV^4 unit. In this figure, we take $\eta_{10} = 6.14$, $N_{\text{eff}} = 3.046$ and $\xi_e = 0$.

In Fig. 5, we show the case of EDE2. We take $\eta_{10} = 6.14$ and $\xi_e = 0$ as in Figs. 3 and 4, but $N_{\text{eff}} = 3.046$ for this case. Since the EDE2 gives a negative contribution to the total energy density of the Universe, which slows down the Hubble expansion rate, the responses of Y_p and D_p to the changes of f_{EDE} and ρ_0 show an opposite tendency to the case of EDE1, i.e., as f_{EDE} and/or ρ_0 increase, the values of Y_p and D_p decrease. However, as in the EDE1 case, the value of Y_p is almost unchanged around the bottom right region in the middle panel where the transition temperature is $T_t \lesssim 0.07$ MeV. As mentioned above, the helium abundance is almost fixed at this temperature, and hence the change of the expansion rate does not affect the final value of Y_p when $T_t < 0.07$ MeV, which is the reason why Y_p stays almost the same as f_{EDE} increases.

Next we show 1σ and 2σ allowed ranges from observations of Y_p [9] and D_p [13] in the $f_{\text{EDE}}-N_{\text{eff}}$ plane in Figs. 6 and 7 for the cases of EDE1 and EDE2, respectively. In the figures, we fix the baryon density to $\eta_{10}^{\text{ref},1}$ and $\eta_{10}^{\text{ref},2}$ as shown in the plots and take several values for ρ_0 which are also indicated in the figure. In all cases, we take the electron neutrino degeneracy parameter as $\xi_e = 0$. From the figure, one can notice that when there is no EDE (i.e., when $f_{\text{EDE}} \rightarrow 0$), there is almost no overlapping region between the allowed ones from the Y_p and D_p measurements in all cases for both EDE1 and EDE2. This is because, as seen from Fig. 1, the allowed regions from Y_p and D_p overlap at $\eta_{10} \sim 5.8$ in the $\eta_{10}-N_{\text{eff}}$ plane when $\xi_e = 0$, but here we fix η_{10} to $\eta_{10}^{\text{ref},1}$ and $\eta_{10}^{\text{ref},2}$, which is larger than $\eta_{10} \sim 5.8$. However, as f_{EDE} increases, the overlapping region between the ones allowed by Y_p and D_p measurements appears, which indicates that EDE can improve the fit.

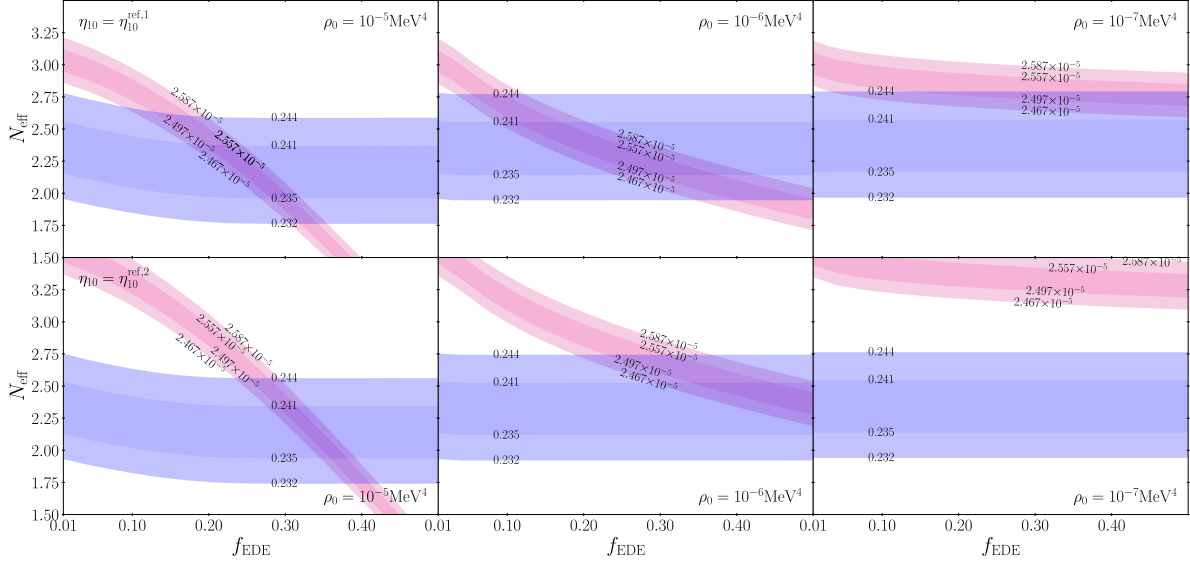


Figure 6: 1σ and 2σ allowed ranges from observations of Y_p [9] (light and dark blue) and D_p [13] (light and dark magenta) in the $f_{\text{EDE}}-N_{\text{eff}}$ plane for EDE1 with $n = 6$. The prior for η_{10} assumed in the analysis is $\eta_{10} = \eta_{10}^{\text{ref},1}$ (top panels) and $\eta_{10}^{\text{ref},2}$ (bottom panels) as shown in the figure. The value of ρ_0 is fixed whose value also appears in the figure. In all panels, the electron neutrino degeneracy parameter is fixed as $\xi_e = 0$.

For the case of EDE1 with the value of ρ_0 shown in the figure, the transition temperature T_t is smaller than 0.07 MeV in most range of f_{EDE} , and hence the value of Y_p scarcely changes even when f_{EDE} is increased as explained above. It should also be noticed that N_{eff} has to be smaller than the standard value ($N_{\text{eff}} = 3.046$) when $\xi_e = 0$ to satisfy the EMPRESS Y_p value as seen from the left panel of Fig. 1. Therefore the region allowed by the Y_p measurement lies below $N_{\text{eff}} = 3.046$ almost horizontally to the axis of f_{EDE} . Contrary to the behavior of Y_p , the deuterium abundance D_p gets smaller as f_{EDE} increases, and hence the overlapping region appears at some value of f_{EDE} , which means that we do not need to assume lepton asymmetry (however, with non-standard value of N_{eff}) when the EDE exists. This holds true for both priors of $\eta_{10}^{\text{ref},1}$ and $\eta_{10}^{\text{ref},2}$ although a large fraction of EDE is required when the baryon density is large (i.e., in the case of the prior of $\eta_{10}^{\text{ref},2}$), which can be noticed by comparing the upper and lower panels in Fig. 6. When ρ_0 is taken to be small, there is no overlapping region due to the small contribution from EDE, particularly for the prior of $\eta_{10}^{\text{ref},2}$.

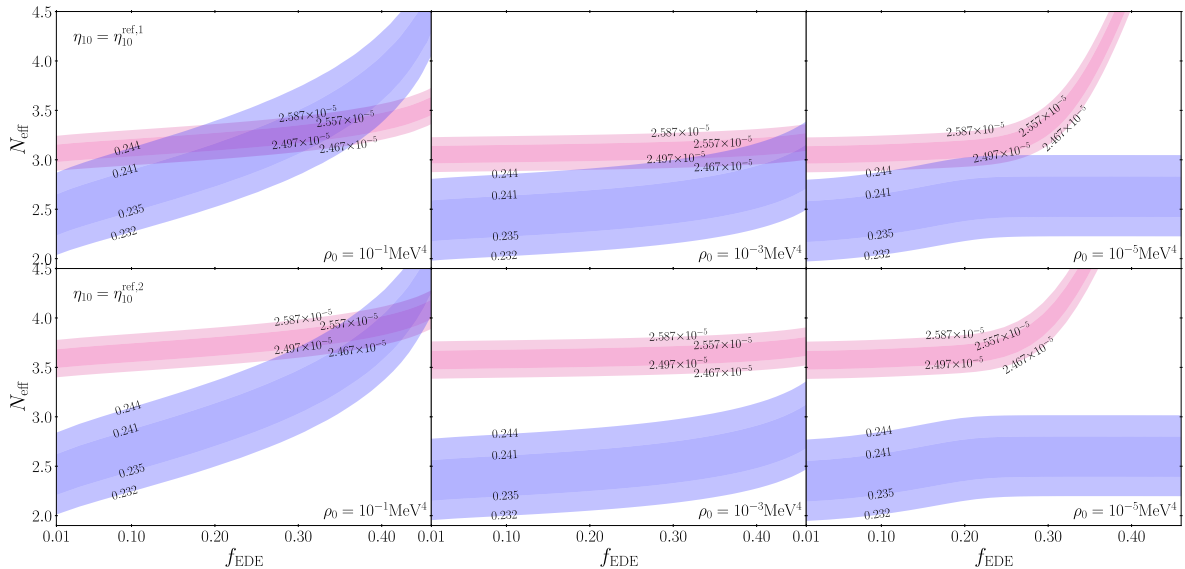


Figure 7: 1σ and 2σ allowed ranges from observations of Y_p [9] (light and dark blue) and D_p [13] (light and dark magenta) in the $f_{\text{EDE}}-N_{\text{eff}}$ plane for EDE2. The prior for η_{10} assumed in the analysis is $\eta_{10} = \eta_{10}^{\text{ref},1}$ (top panels) and $\eta_{10}^{\text{ref},2}$ (bottom panels) as shown in the figure. The value of ρ_0 is fixed whose value also appears in the figure. In all panels, the electron neutrino degeneracy parameter is fixed as $\xi_e = 0$.

In the case of EDE2 shown in Fig. 7, the responses of D_p and Y_p against the increase of f_{EDE} are opposite to those in the EDE1, which is already presented in Fig. 5. However, as in the EDE1 case shown in Fig. 6, the overlapping region between the allowed ones from the Y_p and D_p measurements appears as f_{EDE} increases. It should be noticed that the value of N_{eff} at the overlapping region lies around the standard value for the case of the prior of $\eta_{10} = \eta_{10}^{\text{ref},1}$. This means that the existence of EDE2 can help to fit the EMPRESS Y_p result [9] in combination with the D_p data from [13] without assuming the deviation of N_{eff} from the standard value and with no lepton asymmetry. On the other hand, when a higher baryon density prior $\eta_{10} = \eta_{10}^{\text{ref},2}$ is adopted, having an overlapping region becomes a bit difficult, which can be observed from the lower panels in Fig. 7. Even when such a region exists, the value of N_{eff} is somewhat higher than the standard value. However, we again remark that no lepton asymmetry is assumed in all cases shown in Fig. 7. Thus the EMPRESS Y_p result can be well fitted by assuming the existence of EDE without lepton asymmetry although some non-standard value for N_{eff} could be required, particularly when the baryon density is high.

Next we show constraints from Y_p and D_p in the $\eta_{10}-N_{\text{eff}}$ plane in the presence of EDE with f_{EDE} and ρ_0 being fixed to some values in Fig. 8. EDE1 and EDE2 cases are respectively depicted in left and right panels with $\xi_e = 0$ fixed. For the EDE1 case, we take $f_{\text{EDE}} = 0.09$

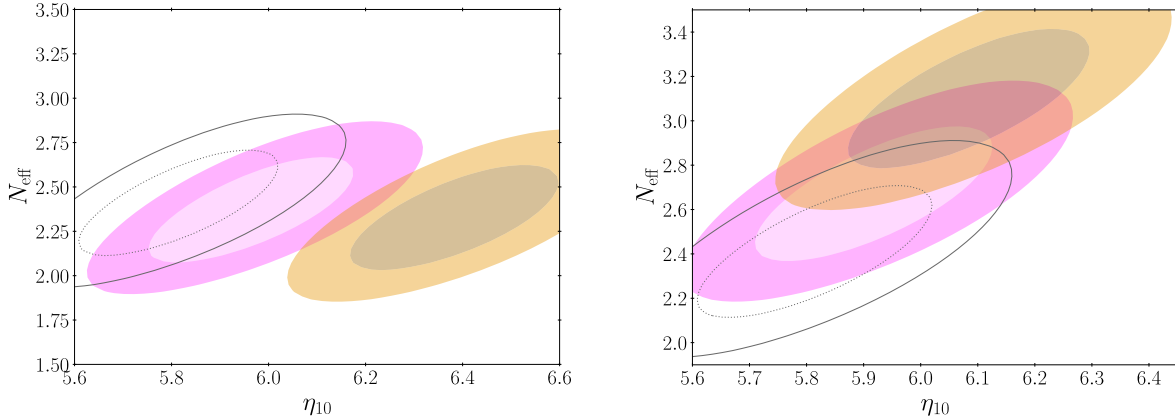


Figure 8: 1σ and 2σ allowed regions in the η_{10} - N_{eff} plane from measurements of Y_p and D_p for the cases of EDE1 (left) and EDE2 (right). In the left panel, we take $\rho_0 = 10^{-6} \text{ MeV}^4$ with $f_{\text{EDE}} = 0.09$ (light and dark magenta for 1σ and 2σ regions) and 0.50 (light and dark orange for 1σ and 2σ regions). In the right panel, we take $\rho_0 = 10^{-2} \text{ MeV}^4$ with $f_{\text{EDE}} = 0.23$ (light and dark magenta for 1σ and 2σ regions) and 0.44 (light and dark orange for 1σ and 2σ regions). For reference, we also show the constraint for the case without EDE with black dotted (1σ) and solid (2σ) lines. In both panels, we assume no lepton asymmetry (i.e., $\xi_e = 0$).

(magenta) and 0.5 (orange) with $\rho_0 = 10^{-6} \text{ MeV}^4$, where light and dark regions respectively correspond to 1σ and 2σ allowed ones. For the EDE2 case, $f_{\text{EDE}} = 0.23$ (magenta) and 0.44 (orange) are assumed with $\rho_0 = 10^{-2} \text{ MeV}^4$.

In the EDE1 case, the deuterium abundance is more affected than that of Y_p , and hence the effect of f_{EDE} degenerates with that of the baryon density since D_p is sensitive to the change of η_{10} . Therefore, as f_{EDE} increases, the allowed region shifts almost horizontally to the right. As discussed in the previous section, when the baryon density is suggested to take a larger value, N_{eff} needs to be larger than the standard case and ξ_e should be (positively) non-zero when no EDE is assumed (see Fig. 1). However, when EDE is present, as the fraction of EDE increases, the allowed region is shifted to a higher value of η_{10} although N_{eff} needs to be smaller than the standard value of $N_{\text{eff}} = 3.046$. Even if the H_0 tension really demands that we need a high value of η_{10} , the EDE1 model can reduce the discrepancy of the baryon density between the EMPRESS Y_p result and CMB with a low value of N_{eff} .

In the case of EDE2, the value of Y_p is decreased by taking a larger value of f_{EDE} , which can cancel the increase of Y_p resulting from a larger value of N_{eff} . Therefore, by appropriately choosing the value of f_{EDE} and ρ_0 , the EDE model can well fit the EMPRESS Y_p [9] and D_p result from [13] simultaneously with the standard value of N_{eff} and without assuming lepton asymmetry when the baryon density is $\eta_{10} \sim 6.14$ which is obtained from the Planck data in the framework of ΛCDM . However, when a higher baryon density is suggested from

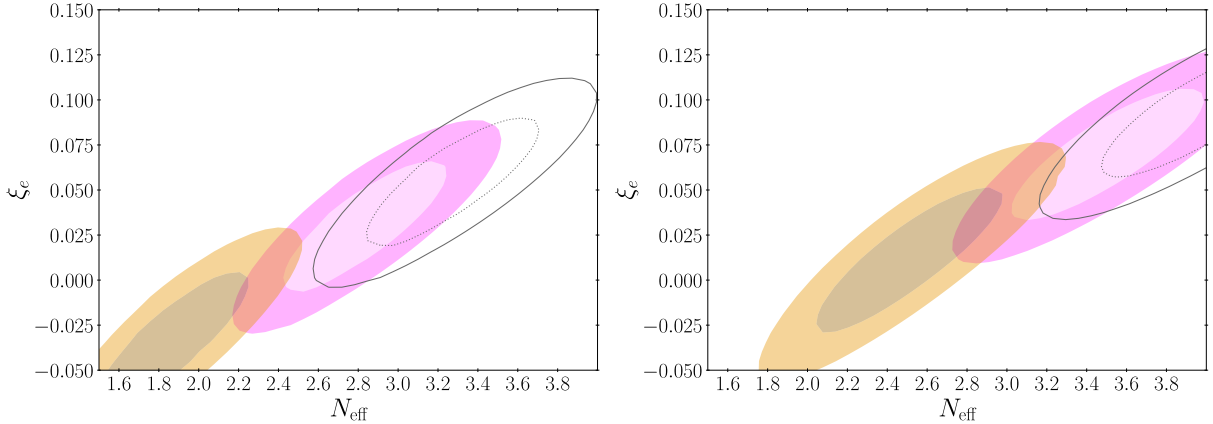


Figure 9: 1σ and 2σ allowed regions in the $N_{\text{eff}}-\xi_e$ plane for the case with EDE1 adopting the priors of $\eta_{10} = \eta_{10}^{\text{ref},1} \pm \sigma_{\eta_{10},1}$ (left) and $\eta_{10} = \eta_{10}^{\text{ref},2} \pm \sigma_{\eta_{10},2}$ (right). We take $f_{\text{EDE}} = 0.09$ (light and dark magenta for 1σ and 2σ regions) and 0.44 (light and dark orange for 1σ and 2σ regions) with $\rho_0 = 10^{-6} \text{ MeV}^4$. For reference, we also show the constraint for the case without EDE with black dotted (1σ) and solid (2σ) lines.

CMB, which could be motivated in the light of the H_0 tension, one needs a larger value of N_{eff} than the standard one. When $\eta_{10} \sim 6.4$, the EDE2 model with $f_{\text{EDE}} = 0.44$ and $\rho_0 = 8 \times 10^{-2} \text{ MeV}^4$ can be well fitted to the data, but with $N_{\text{eff}} = 4.0$. In any case, the existence of EDE can help to improve the fit to the EMPRESS Y_p result without resorting to lepton asymmetry even if a higher baryon density is suggested.

Finally, we discuss constraints in the $N_{\text{eff}}-\xi_e$ plane. 1σ and 2σ allowed regions are shown for the cases of EDE1 and EDE2 in Figs. 9 and 10, respectively. In each figure, two priors for η_{10} , i.e., $\eta_{10} = \eta_{10}^{\text{ref},1} \pm \sigma_{\eta_{10},1}$ and $\eta_{10}^{\text{ref},2} \pm \sigma_{\eta_{10},2}$, are adopted, which are respectively shown in left and right panels in the figures. For reference, we also show the constraints for the case without EDE.

In the case of the EDE1 shown in Fig. 9, we take $f_{\text{EDE}} = 0.09$ (magenta) and 0.44 (orange) with $\rho_0 = 10^{-6} \text{ MeV}^4$, where light and dark regions correspond to 1σ and 2σ allowed ones, respectively. Since larger f_{EDE} gives larger Y_p and D_p , the decrease of N_{eff} and ξ_e are canceled by a large value of f_{EDE} and hence the allowed region shifts to a lower left direction by raising f_{EDE} . Although the standard point with $N_{\text{eff}} = 3.046$ and $\xi_e = 0$ is a bit away from 2σ bound for the prior of both $\eta_{10}^{\text{ref},1}$ and $\eta_{10}^{\text{ref},2}$, either $N_{\text{eff}} = 3.046$ or $\xi_e = 0$ can be realized by appropriately choosing the value of f_{EDE} and ρ_0 in the EDE1 case. Notice that this holds true even if the prior of a large baryon density $\eta_{10}^{\text{ref},2}$ is adopted where a more deviation from the standard values for both N_{eff} and ξ_e are required to fit the EMPRESS Y_p result without EDE.

In the case of the EDE2 which is depicted in Fig. 10, we assume $f_{\text{EDE}} = 0.17$ (magenta) and 0.44 (orange) in left panel. In the right panel, $f_{\text{EDE}} = 0.41$ (magenta) and 0.47 (orange)

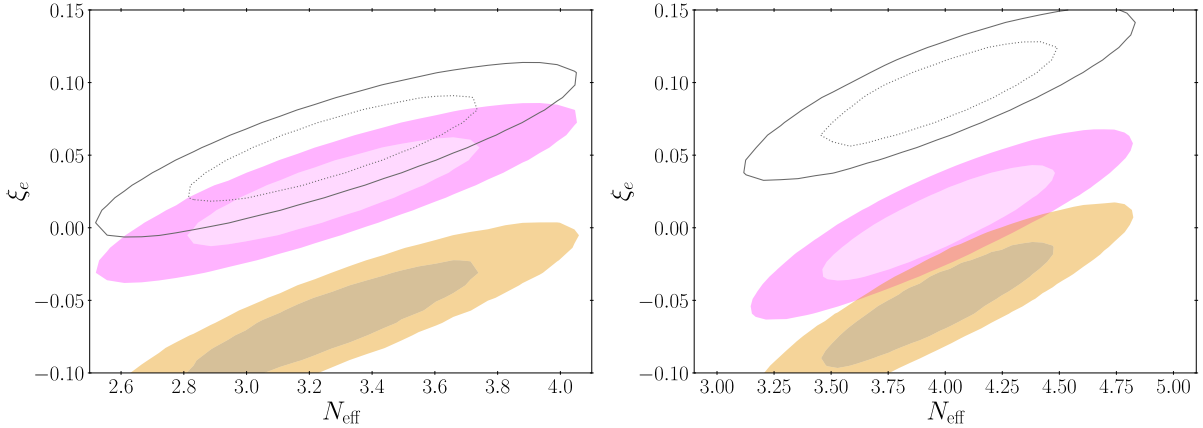


Figure 10: 1σ and 2σ allowed regions in the $N_{\text{eff}}-\xi_e$ plane for the case with the EDE2, adopting the priors of $\eta_{10} = \eta_{10}^{\text{ref},1} \pm \sigma_{\eta_{10},1}$ (left) and $\eta_{10} = \eta_{10}^{\text{ref},2} \pm \sigma_{\eta_{10},2}$ (right). In the left panel, we take $f_{\text{EDE}} = 0.17$ (light and dark magenta for 1σ and 2σ regions) and 0.44 (light and dark orange for 1σ and 2σ regions). In the right panel, we take $f_{\text{EDE}} = 0.41$ (light and dark magenta for 1σ and 2σ regions) and 0.47 (light and dark orange for 1σ and 2σ regions). In both panels, ρ_0 is assumed as $\rho_0 = 10^{-1} \text{ MeV}^4$. For reference, we also show the constraint for the case without EDE with black dotted (1σ) and solid (2σ) lines.

are assumed. In both panels, we take $\rho_0 = 10^{-1} \text{ MeV}^4$. As can be noticed from the figure, by changing the values of f_{EDE} and ρ_0 , the allowed region in the $N_{\text{eff}}-\xi_e$ plane moves almost vertically downwards. One can see that, when the baryon density is $\eta_{10} \sim 6.14$, the standard value of N_{eff} with no lepton asymmetry can be well fitted to the EMPRESS Y_p result in the presence of EDE with appropriately chosen f_{EDE} and ρ_0 . On the other hand, when a high baryon density prior of $\eta_{10}^{\text{ref},2}$ is adopted, the EMPRESS result demands the value of N_{eff} higher than the standard one even assuming the presence of EDE. However, it should be emphasized that both a high value of N_{eff} and positively non-zero ξ_e are required to fit the EMPRESS Y_p result when EDE is absent, which can be seen from the right panel of Fig. 2, on the other hand, once we assume EDE, one can fit the EMPRESS Y_p without any lepton asymmetry, which indicates that EDE can mitigate the helium anomaly caused by the EMPRESS Y_p results.

4 Conclusion and Discussion

In this paper, first we have investigated the impact of the H_0 tension, in which a higher value of baryon density could be preferred than in the ΛCDM framework, on BBN in the light of recent Y_p measurement by EMPRESS. As already pointed out [9], the EMPRESS Y_p result would infer a value of N_{eff} higher than the standard case and a positively non-zero value of

ξ_e . However, given that models proposed to resolve the H_0 tension tend to prefer a higher baryon density than that in the Λ CDM adopted in [9], the deviation from the standard assumption ($N_{\text{eff}} = 3.046$ and $\xi_e = 0$) would be more significant. As shown in Figs. 1 and 2, when a large η_{10} is assumed, which is suggested by the H_0 tension, N_{eff} needs to be much larger than the standard value of $N_{\text{eff}} = 3.046$ and ξ_e should take a large positively non-zero value to explain the EMPRESS Y_p value in combination with the D_p measurement of [13]. Therefore, the H_0 tension could also affect BBN, which shows that the tension would have a further impact on other aspects of cosmology.

We have also studied the effects of early dark energy, which has been extensively investigated in the context of the H_0 tension, on the abundances of helium and deuterium. As mentioned above, the EMPRESS Y_p results suggest that non-standard values of N_{eff} and non-zero ξ_e are necessary to have a good fit to Y_p and D_p data simultaneously, however, by assuming the existence of early dark energy whose energy density can have a sizable fraction during BBN, the values of N_{eff} and/or ξ_e can still take the standard values, depending on the EDE model and parameters. Even if a larger value of η_{10} is assumed, which could be demanded by models resolving the H_0 tension, the existence of early dark energy can still reduce the tension such that N_{eff} and/or ξ_e can take the values close to the standard ones. Therefore early dark energy can improve the fit even in the case of a large baryon density in the light of the EMPRESS Y_p results.

The recent EMPRESS results may suggest physics beyond the standard cosmological model. By taking account of the H_0 tension, which is one of the most significant tensions in cosmology today, the modification/extension of the standard model could be more in demand. Our study may indicate that the tensions in cosmology should be simultaneously investigated in order to pursue a new cosmological model, from which one can have a profound insight not only into the evolution of the Universe but also on into the fundamental physics.

Acknowledgements

The work of T.T. was supported by JSPS KAKENHI Grant Number 19K03874.

References

- [1] A. G. Riess et al., *A Comprehensive Measurement of the Local Value of the Hubble Constant with 1 km/s/Mpc Uncertainty from the Hubble Space Telescope and the SH0ES Team*, [arXiv:2112.04510](#).
- [2] **Planck** Collaboration, N. Aghanim et al., *Planck 2018 results. VI. Cosmological parameters*, *Astron. Astrophys.* **641** (2020) A6, [[arXiv:1807.06209](#)]. [Erratum: *Astron.Astrophys.* 652, C4 (2021)].
- [3] N. Schöneberg, J. Lesgourgues, and D. C. Hooper, *The BAO+BBN take on the Hubble tension*, *JCAP* **10** (2019) 029, [[arXiv:1907.11594](#)].
- [4] F. Okamoto, T. Sekiguchi, and T. Takahashi, *H_0 tension without CMB data: Beyond the Λ CDM*, *Phys. Rev. D* **104** (2021), no. 2 023523, [[arXiv:2105.12312](#)].
- [5] N. Schöneberg, L. Verde, H. Gil-Marín, and S. Brieden, *BAO+BBN revisited – Growing the Hubble tension with a 0.7km/s/Mpc constraint*, [arXiv:2209.14330](#).
- [6] E. Di Valentino, O. Mena, S. Pan, L. Visinelli, W. Yang, A. Melchiorri, D. F. Mota, A. G. Riess, and J. Silk, *In the realm of the Hubble tension—a review of solutions*, *Class. Quant. Grav.* **38** (2021), no. 15 153001, [[arXiv:2103.01183](#)].
- [7] L. Perivolaropoulos and F. Skara, *Challenges for Λ CDM: An update*, *New Astron. Rev.* **95** (2022) [[arXiv:2105.05208](#)].
- [8] N. Schöneberg, G. Franco Abellán, A. Pérez Sánchez, S. J. Witte, V. Poulin, and J. Lesgourgues, *The H_0 Olympics: A fair ranking of proposed models*, *Phys. Rept.* **984** (2022) 1–55, [[arXiv:2107.10291](#)].
- [9] A. Matsumoto et al., *EMPRESS. VIII. A New Determination of Primordial He Abundance with Extremely Metal-Poor Galaxies: A Suggestion of the Lepton Asymmetry and Implications for the Hubble Tension*, [arXiv:2203.09617](#).
- [10] E. Aver, K. A. Olive, and E. D. Skillman, *The effects of He I λ 10830 on helium abundance determinations*, *JCAP* **07** (2015) 011, [[arXiv:1503.08146](#)].
- [11] T. Hsyu, R. J. Cooke, J. X. Prochaska, and M. Bolte, *The PHLEK Survey: A New Determination of the Primordial Helium Abundance*, *Astrophys. J.* **896** (2020), no. 1 77, [[arXiv:2005.12290](#)].
- [12] O. A. Kurichin, P. A. Kislitsyn, V. V. Klimenko, S. A. Balashev, and A. V. Ivanchik, *A new determination of the primordial helium abundance using the analyses of H II region spectra from SDSS*, *Mon. Not. Roy. Astron. Soc.* **502** (2021), no. 2 3045–3056, [[arXiv:2101.09127](#)].

- [13] R. J. Cooke, M. Pettini, and C. C. Steidel, *One Percent Determination of the Primordial Deuterium Abundance*, *Astrophys. J.* **855** (2018), no. 2 102, [[arXiv:1710.11129](#)].
- [14] G. Mangano, G. Miele, S. Pastor, T. Pinto, O. Pisanti, and P. D. Serpico, *Relic neutrino decoupling including flavor oscillations*, *Nucl. Phys. B* **729** (2005) 221–234, [[hep-ph/0506164](#)].
- [15] P. F. de Salas and S. Pastor, *Relic neutrino decoupling with flavour oscillations revisited*, *JCAP* **07** (2016) 051, [[arXiv:1606.06986](#)].
- [16] M. Escudero Abenza, *Precision early universe thermodynamics made simple: N_{eff} and neutrino decoupling in the Standard Model and beyond*, *JCAP* **05** (2020) 048, [[arXiv:2001.04466](#)].
- [17] K. Akita and M. Yamaguchi, *A precision calculation of relic neutrino decoupling*, *JCAP* **08** (2020) 012, [[arXiv:2005.07047](#)].
- [18] J. Froustey, C. Pitrou, and M. C. Volpe, *Neutrino decoupling including flavour oscillations and primordial nucleosynthesis*, *JCAP* **12** (2020) 015, [[arXiv:2008.01074](#)].
- [19] J. J. Bennett, G. Buldgen, P. F. De Salas, M. Drewes, S. Gariazzo, S. Pastor, and Y. Y. Y. Wong, *Towards a precision calculation of N_{eff} in the Standard Model II: Neutrino decoupling in the presence of flavour oscillations and finite-temperature QED*, *JCAP* **04** (2021) 073, [[arXiv:2012.02726](#)].
- [20] O. Seto and Y. Toda, *Hubble tension in lepton asymmetric cosmology with an extra radiation*, *Phys. Rev. D* **104** (2021), no. 6 063019, [[arXiv:2104.04381](#)].
- [21] M. Kawasaki and K. Murai, *Lepton asymmetric universe*, *JCAP* **08** (2022), no. 08 041, [[arXiv:2203.09713](#)].
- [22] A.-K. Burns, T. M. P. Tait, and M. Valli, *Indications for a Nonzero Lepton Asymmetry in the Early Universe*, [arXiv:2206.00693](#).
- [23] D. Borah and A. Dasgupta, *Large Neutrino Asymmetry from TeV Scale Leptogenesis in the Light of Helium Anomaly*, [arXiv:2206.14722](#).
- [24] M. Escudero, A. Ibarra, and V. Maura, *Primordial Lepton Asymmetries in the Precision Cosmology Era: Current Status and Future Sensitivities from BBN and the CMB*, [arXiv:2208.03201](#).
- [25] K. Kohri and K.-i. Maeda, *A possible solution to the helium anomaly of EMPRESS VIII by cuscuton gravity theory*, *PTEP* **2022** (2022), no. 9 091E01, [[arXiv:2206.11257](#)].

- [26] V. Poulin, T. L. Smith, T. Karwal, and M. Kamionkowski, *Early Dark Energy Can Resolve The Hubble Tension*, *Phys. Rev. Lett.* **122** (2019), no. 22 221301, [[arXiv:1811.04083](#)].
- [27] T. Sekiguchi and T. Takahashi, *Cosmological bound on neutrino masses in the light of H_0 tension*, *Phys. Rev. D* **103** (2021), no. 8 083516, [[arXiv:2011.14481](#)].
- [28] G. Ye, B. Hu, and Y.-S. Piao, *Implication of the Hubble tension for the primordial Universe in light of recent cosmological data*, *Phys. Rev. D* **104** (2021), no. 6 063510, [[arXiv:2103.09729](#)].
- [29] F. Takahashi and W. Yin, *Cosmological implications of $n_s \approx 1$ in light of the Hubble tension*, *Phys. Lett. B* **830** (2022) 137143, [[arXiv:2112.06710](#)].
- [30] J.-Q. Jiang and Y.-S. Piao, *Toward early dark energy and $n_s=1$ with Planck, ACT, and SPT observations*, *Phys. Rev. D* **105** (2022), no. 10 103514, [[arXiv:2202.13379](#)].
- [31] G. Ye, J.-Q. Jiang, and Y.-S. Piao, *Towards hybrid inflation with $n_s = 1$ in light of Hubble tension and primordial gravitational waves*, [arXiv:2205.02478](#).
- [32] K. Ichikawa, T. Sekiguchi, and T. Takahashi, *Primordial Helium Abundance from CMB: a constraint from recent observations and a forecast*, *Phys. Rev. D* **78** (2008) 043509, [[arXiv:0712.4327](#)].
- [33] K. Ichikawa, T. Sekiguchi, and T. Takahashi, *Probing the Effective Number of Neutrino Species with Cosmic Microwave Background*, *Phys. Rev. D* **78** (2008) 083526, [[arXiv:0803.0889](#)].
- [34] T. Sekiguchi and T. Takahashi, *Early recombination as a solution to the H_0 tension*, *Phys. Rev. D* **103** (2021), no. 8 083507, [[arXiv:2007.03381](#)].
- [35] G. Ye and Y.-S. Piao, *Is the Hubble tension a hint of AdS phase around recombination?*, *Phys. Rev. D* **101** (2020), no. 8 083507, [[arXiv:2001.02451](#)].
- [36] J. C. Hill, E. McDonough, M. W. Toomey, and S. Alexander, *Early dark energy does not restore cosmological concordance*, *Phys. Rev. D* **102** (2020), no. 4 043507, [[arXiv:2003.07355](#)].
- [37] F. Niedermann and M. S. Sloth, *Resolving the Hubble tension with new early dark energy*, *Phys. Rev. D* **102** (2020), no. 6 063527, [[arXiv:2006.06686](#)].
- [38] M. Braglia, M. Ballardini, F. Finelli, and K. Koyama, *Early modified gravity in light of the H_0 tension and LSS data*, *Phys. Rev. D* **103** (2021), no. 4 043528, [[arXiv:2011.12934](#)].
- [39] K. Jedamzik and L. Pogosian, *Relieving the Hubble tension with primordial magnetic fields*, *Phys. Rev. Lett.* **125** (2020), no. 18 181302, [[arXiv:2004.09487](#)].

- [40] M. Escudero and S. J. Witte, *The hubble tension as a hint of leptogenesis and neutrino mass generation*, *Eur. Phys. J. C* **81** (2021), no. 6 515, [[arXiv:2103.03249](#)].
- [41] R. Consiglio, P. F. de Salas, G. Mangano, G. Miele, S. Pastor, and O. Pisanti, *PARthENoPE reloaded*, *Comput. Phys. Commun.* **233** (2018) 237–242, [[arXiv:1712.04378](#)].
- [42] P. D. Serpico, S. Esposito, F. Iocco, G. Mangano, G. Miele, and O. Pisanti, *Nuclear reaction network for primordial nucleosynthesis: A Detailed analysis of rates, uncertainties and light nuclei yields*, *JCAP* **12** (2004) 010, [[astro-ph/0408076](#)].
- [43] G. Steigman, *The Cosmological Evolution of the Average Mass Per Baryon*, *JCAP* **10** (2006) 016, [[astro-ph/0606206](#)].
- [44] O. Pisanti, A. Cirillo, S. Esposito, F. Iocco, G. Mangano, G. Miele, and P. D. Serpico, *PARthENoPE: Public Algorithm Evaluating the Nucleosynthesis of Primordial Elements*, *Comput. Phys. Commun.* **178** (2008) 956–971, [[arXiv:0705.0290](#)].
- [45] S. Gariazzo, P. F. de Salas, O. Pisanti, and R. Consiglio, *PARthENoPE revolutions*, *Comput. Phys. Commun.* **271** (2022) 108205, [[arXiv:2103.05027](#)].
- [46] K. Kohri, M. Kawasaki, and K. Sato, *Big bang nucleosynthesis and lepton number asymmetry in the universe*, *Astrophys. J.* **490** (1997) 72–75, [[astro-ph/9612237](#)].
- [47] **Particle Data Group** Collaboration, P. A. Zyla et al., *Review of Particle Physics*, *PTEP* **2020** (2020), no. 8 083C01.
- [48] K. Freese and M. W. Winkler, *Chain early dark energy: A Proposal for solving the Hubble tension and explaining today’s dark energy*, *Phys. Rev. D* **104** (2021), no. 8 083533, [[arXiv:2102.13655](#)].
- [49] K. Rezazadeh, A. Ashoorioon, and D. Grin, *Cascading Dark Energy*, [[arXiv:2208.07631](#)].
- [50] E. Mörtzell and S. Dhawan, *Does the Hubble constant tension call for new physics?*, *JCAP* **09** (2018) 025, [[arXiv:1801.07260](#)].
- [51] V. Poulin, K. K. Boddy, S. Bird, and M. Kamionkowski, *Implications of an extended dark energy cosmology with massive neutrinos for cosmological tensions*, *Phys. Rev. D* **97** (2018), no. 12 123504, [[arXiv:1803.02474](#)].
- [52] **BOSS** Collaboration, T. Delubac et al., *Baryon acoustic oscillations in the Ly α forest of BOSS DR11 quasars*, *Astron. Astrophys.* **574** (2015) A59, [[arXiv:1404.1801](#)].
- [53] E. Aubourg et al., *Cosmological implications of baryon acoustic oscillation measurements*, *Phys. Rev. D* **92** (2015), no. 12 123516, [[arXiv:1411.1074](#)].

- [54] H. du Mas des Bourboux et al., *Baryon acoustic oscillations from the complete SDSS-III Ly α -quasar cross-correlation function at $z = 2.4$* , *Astron. Astrophys.* **608** (2017) A130, [[arXiv:1708.02225](#)].
- [55] H. du Mas des Bourboux et al., *The Completed SDSS-IV Extended Baryon Oscillation Spectroscopic Survey: Baryon Acoustic Oscillations with Ly α Forests*, *Astrophys. J.* **901** (2020), no. 2 153, [[arXiv:2007.08995](#)].
- [56] Y. Wang, L. Pogosian, G.-B. Zhao, and A. Zucca, *Evolution of dark energy reconstructed from the latest observations*, *Astrophys. J. Lett.* **869** (2018) L8, [[arXiv:1807.03772](#)].
- [57] K. Dutta, Ruchika, A. Roy, A. A. Sen, and M. M. Sheikh-Jabbari, *Beyond Λ CDM with low and high redshift data: implications for dark energy*, *Gen. Rel. Grav.* **52** (2020), no. 2 15, [[arXiv:1808.06623](#)].
- [58] M. Fasiello and A. J. Tolley, *Cosmological Stability Bound in Massive Gravity and Bigravity*, *JCAP* **12** (2013) 002, [[arXiv:1308.1647](#)].
- [59] Y. Akrami, S. F. Hassan, F. Könnig, A. Schmidt-May, and A. R. Solomon, *Bimetric gravity is cosmologically viable*, *Phys. Lett. B* **748** (2015) 37–44, [[arXiv:1503.07521](#)].
- [60] F. Könnig, *Higuchi Ghosts and Gradient Instabilities in Bimetric Gravity*, *Phys. Rev. D* **91** (2015) 104019, [[arXiv:1503.07436](#)].
- [61] O. Akarsu, J. D. Barrow, L. A. Escamilla, and J. A. Vazquez, *Graduated dark energy: Observational hints of a spontaneous sign switch in the cosmological constant*, *Phys. Rev. D* **101** (2020), no. 6 063528, [[arXiv:1912.08751](#)].
- [62] O. Akarsu, S. Kumar, E. Özulker, and J. A. Vazquez, *Relaxing cosmological tensions with a sign switching cosmological constant*, *Phys. Rev. D* **104** (2021), no. 12 123512, [[arXiv:2108.09239](#)].
- [63] O. Akarsu, S. Kumar, E. Ozulker, J. A. Vazquez, and A. Yadav, *Relaxing cosmological tensions with a sign switching cosmological constant: Improved results with Planck, BAO and Pantheon data*, [[arXiv:2211.05742](#)].
- [64] M. Ahmed, S. Dodelson, P. B. Greene, and R. Sorkin, *Everpresent Λ* , *Phys. Rev. D* **69** (2004) 103523, [[astro-ph/0209274](#)].
- [65] N. Zwane, N. Afshordi, and R. D. Sorkin, *Cosmological tests of Everpresent Λ* , *Class. Quant. Grav.* **35** (2018), no. 19 194002, [[arXiv:1703.06265](#)].